VARIATION OF EFFECTIVE STRESS RANGE RATIO UNDER SIMPLE VARIABLE AMPLITUDE LOADING

S. Chand and S. B. L. Garg

Mechanical Engineering Department, M.N.R. Engineering College, Allahabad 211004, India

ABSTRACT

The models for the effective stress range ratio, U are developed from observed crack closure data for different simple variable Amplitude loadings (VAL) . These models of U are used in Constant Amplitude Load (CAL) crack growth rate (CGR) law to find CGRS for VAL. These computed results are later compared with the observed results.

KEY WORDS

Crack growth rates; effective stress range ratio; affecting zone; stress ratio; constant amplitude load; variable amplitude loads; peak high load cycle.

INTRODUCTION

In space vehicles and air craft structures, during service, the loading is often complex. The CGRS depend upon the past load history. As reported in literature (Jones, 1973; Mills and Hertzberg, 1976; VonEuw and Hertzberg, 1972), the CAL- CGR laws should consider the effect of following four factors, to make them applicable to complex type of loading.

1. Strain hardening exponent, 2. Crack tip blunting, 3. Residual stress in plastic zone, 4. Residual deformations at the crack tip as a result of past load history.

The effect of strain hardening exponent (n) is considered in deriving CAL-CGR law (Chand and Garg, 1983 b), given by eqn. (1). The residual stresses and residual deformations in the wake of crack tip manifest their effect in influencing the phenomena of crack closure (Buck, Frandsen and Marcus, 1976), which is considered in U-parameter defined by Elber (1971). In the absence of suitable measurement technique for measuring crack tip radii, the effect of crack tip blunting is not considered. Thus, the aim of present work is to find how far, the present model, considering the effect of remaining three parameters, is able to give the CGRS in VAL.

EXPERIMENTAL PROCEDURE

The crack propagation experiments, for different load patterns given in table-1 were performed on subresonant type of push- pull fatigue machine at 25 Hz on centrally notched test specimens of 6063-T6 Al-alloy having a width of 63.5 mm and thickness of 3.15 mm. The composition and properties of this material are given in publications of Chand and Garg (1983a, 1983b). The position of crack tip was noted with the help of travelling microscope with an accuracy of 0.02 mm using stroboscopic light. For each type of loading, three specimens were tested to find crack growth rate data, while crack closure experiments were performed on one of them only. To get crack closure load data, load displacement curves were recorded at various crack lengths during CGR experiments on X - Y recorder using small COD-gauge (Chand and Garg, 1983a). The gauge signal was amplified with a d.c. amplifier. The gauge was placed across the crack, 3 mm behind the crack tip. The load-displacement records were taken by unloading the test specimens statically from maximum load to minimum or zero load. The records for all the load patterns are presented in reference of Chand and Garg (1983c). Knowing the crack closure loads from these records, the values of U were found from eqn. (2). In developing U- models, the values of U were found having the magnitude less and more than unity for reasons explained in ref. (Chand and Garg, 1983a).

$$da/dN = C \ (U\Delta K)^2 \ \sigma_y \ /nE \ K_{Ic}^2 \ (1+R)^{3.8}, \ \text{where } C = 0.15 mm \qquad (1)$$

$$U = (\sigma_{max} - \sigma_{cl}) / (\sigma_{max} - \sigma_{min}) \qquad (2)$$

DEVELOPMENT OF U-MODELS

Here U-models developed are for the affecting zone (a_{O2}^* -created by P_0-P_2 load range at a_c -crack length at which load is changed) for different load patterns. Upto the begining of the affecting zone and after the crack crosses this zone, the CAL- U model (eqn 3) is applicable. The value of a_{O2}^* is almost equal to plane stress plastic zone (Chand and Garg, 1983c) given by eqn (4). Few more terms, which will appear in the text are U_{CO1} and U_{EO1}- these are CAL-U values at points C and E i.e. at the begining and end of the affecting zone created by load range P_0-P_1. The stress ratio terms R_{O1} and R_{O2} correspond to load ranges P_0- P_1 and P_0- P_2 (table 1) respectively. Lastly the term K_{O2} correspond to stress intensity factor for P_0- P_2 load range. The other terms have their usual meanings. The values of U obtained within the affecting zone are plotted w.r.t. crack length, a, and on log-log paper w.r.t.(X/a_{O2}^*) in

TABLE 1 Different Load Patterns

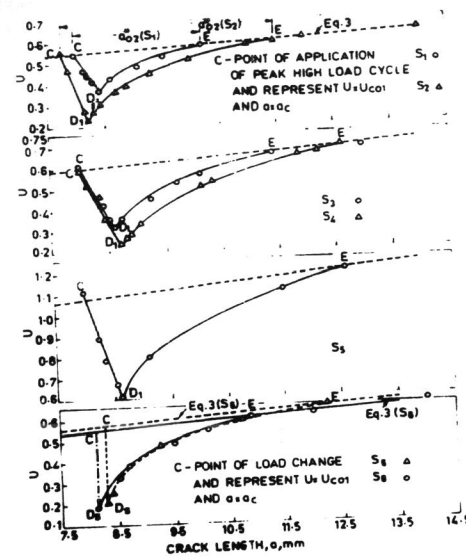| LOAD PATERN	TEST (a_c)	P_o	$\dfrac{P_o}{P_1}$	$\dfrac{P_2}{P_1}$	LOAD PATTERN	TEST (a_c)	$\dfrac{P_o}{(P_o')}$	$\dfrac{P_o}{P_1}$	$\dfrac{P_2}{P_1}$
	S_1 (8·0)	120	0·10	1·50		S_6 (8·26)	136·8 (-)		
	S_2 (7·75)	120	0·10	2·0		S_7 (8·10)	136·8 (-)	0·10	1·75
	S_3 (8·0)	150	0·10	1·50					
	S_4 (8·0)	150	0·10	1·75		S_8 (8·10)	126·6 (760)	0·40	1·5
	S_5 (8·10)	600	0·40	1·75					

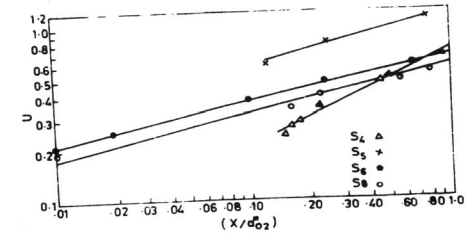Fig. 1a Variation of U w.r.t. crack length

Fig. 1b Variation of U w.r.t.(X/a_{O2}^*)

Figs.1, where $X = (a - a_c)$. The development of U-models for different load patterns is explained under different headings given below.

$$U = (6 + 8.8 R) \ \Delta K / \ (1-R) \ . \ 1000 + 1.30 \ R + 0.20 \qquad (3)$$

$$W = (K_{O2}^2 \ / \ \Pi \ \sigma_y^2) \qquad (4)$$

Intermediate single peak high load cycle (PHLC) in CAL-test(S_1 to S_5). Just after the application of PHLC, accelerated values of U were observed by Chand and Garg (1983c), which are ignored for the U-model development. The plots of U (Figs. 1a), show that after the application of PHLC at point C, the values of U decrease linearly with increase in a upto D_1, thereafter, U starts to increase with further increase in a and merges with CAL-U (eqn.3) at E. The value of X (= a-a_c) at D_1 has been expressed as (Z_1 a_{O2}^*), where Z_1 is found to lie between 0.12 to 0.17. The plot of U w.r.t. (X/a_{O2}^*) on log-log paper between D_1 and E show linear variation (Fig. 1b). By curve fitting method, following expressions of U (eqns.5) are obtained.

$$U = (U_{EO1} \ Z_1^q - U_{CO1}). \ X/(Z_1 \ a_{O2}^*)+ U_{CO1}, \ 0 \leqslant (X/a_{O2}^*) \leqslant Z_1 \qquad (5a)$$

$$U = U_{EO1} \ (X/a_{O2}^*)^q, \ Z_1 \leqslant \ (X/a_{O2}^*) \leqslant 1 \qquad (5b)$$

$$\text{where } q = 0.12 \ a_{O2}^* \ (1+ R_{O2}/1+ R_{O1})^2$$

Hi-Lo load sequence tests and decrease in mean load sequence tests (S_6, S_8). The variation of U (Figs.1) for both these tests show that after load change at C, the values of U abruptly decrease to a minimum value (from C to D_8), without showing delayed retardation. On further increase in a, U starts to increase and approaches CAL-U value (P_0- P_1) at E. Further U Vs (X/a_{O2}^*)

plots on log-log paper show straight line. To avoid singularity, the minimum value is assumed to occur at $X = 0.01\ a^*_{02}$ instead of $X = 0$. The equation which fits the experimental data is given below (eqn. 6).

$$U = U_{EO1}(X/a^*_{02})^q,\ 0.01 \leqslant (X/a^*_{02}) \leqslant 1 \qquad (6)$$

where $q = 0.07\ a^*_{02}\ (1 + R_{02} / 1 + R_{01})^2$

Intermediate multi PHLC applied in CAL-test. Literature studies by Bell and Creager (1974) have shown that same magnitude of retardation is obtained in Hi-Lo load sequence test, as after applying a particular number - named as saturated number (Ns) of multi PHLC in a CAL- test. The variation of U within affecting zone for single PHLC and Hi-Lo load sequence is schematically shown (Fig. 2) by CD_1E and CD_SE respectively. The values of U and Z at points D_1 and D_S are named as U_1, U_S, Z_1 and Z_S respectively. It is assumed that for any number of multi PHLC (N_{PH}) U and Z are named as U_N and Z_N. The U-models given by eqns.(5) and (6) are extrapolated for any number, N_{PH} lying between 1 and N_S assuming linear variation of U_1 to U_S and Z_1 to Z_S as N_{PH} vary from 1 to N_S. On the basis of above, the U- models are given by eqns.(7). These models for $N_{PH} = 1$ and N_S become the same as eqns (5) and (6) respectively.

$$U = (U_{EO1}\ Z^q_N - U_{CO1})X/(Z_N\ a^*_{02}) + U_{CO1},\ 0 \leqslant (X/a^*_{02}) \leqslant Z_N, 1 \leqslant N \leqslant N_S \qquad (7a)$$

$$U = U_{EO1}(X/a^*_{02})^q,\ Z_N \leqslant (X/a^*_{02}) \leqslant 1,\ 1 \leqslant N \leqslant N_S \qquad (7b)$$

where $q = \log_e(U_N / U_{EO1})\ /\log_e Z_N$

$$Z_N = [\ Z_1(N_{PH} - N_S) - Z_S\ (\ N_{PH} - 1)]\ /(1 - N_S)$$

$$U_N = [\ U_1(N_{PH} - N_S) - U_S\ (\ N_{PH} - 1)]\ /\ (1 - N_S)$$

Lo-Hi load sequence test (S_7). Because of the use of subresonant machine, sufficient amount of crack grew during load adjustment. Therefore, the crack closure load data recorded is insufficient to develop U model. The model of Hi-Lo load sequence is modified in accordance with the CGR trend of this test. As visible from CGR trend of Lo-Hi load sequence test (Fig.9), the value of U is expected to become maximum just after load change, while the same in Hi-Lo load test (S_6) is minimum (Figs.1a). On the basis of these arguments, in U model of Hi-Lo load sequence (eqn.6), U_{EO1} is replaced by U_{EO2} and q by - q. The final model of U for Lo-Hi load test is given below (eqn. 8).

$$U = U_{EO2}(X/a^*_{02})^{-q},\ .01 \leqslant (X/a^*_{02}) \leqslant a \qquad (8)$$

where $q = 0.07\ a^*_{02}\ (\ 1 + R_{02} / 1 + R_{01})^2$

The results of U-models given by eqns. (5),(6) and (8) agree within $\pm 6\%$ with the experimental data (Fig.3).

COMPARISON OF CGR- MODEL RESULTS WITH EXPERIMENTAL RESULTS

The comparision of computed crack growth rates and a/N curves found, using present model with experimental results is discussed below. To compute a/N curve, the affecting zone is divided in 50 small zones and CGRS are found at the ends of each zone. The average of these two CGRS is used to find the number of cycles required to traverse the small zone. The region outside the affecting zone is divided in the zones of 0.25 mm and CAl- formulae are used.

Intermediate single PHLC in CAL tests (S_1 to S_5). For S_1 to S_4 tests(Figs.4a and 4b), it is observed that just after the application of PHLC, the model CGR results are observed to be close to the experimental data. But as ΔK (or a)
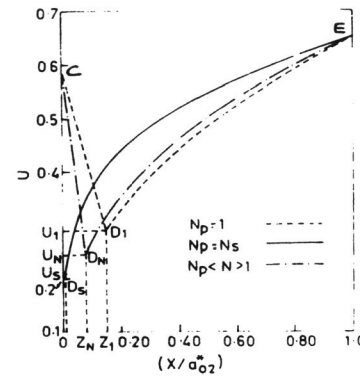

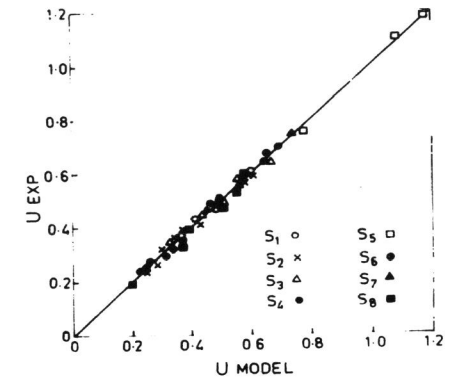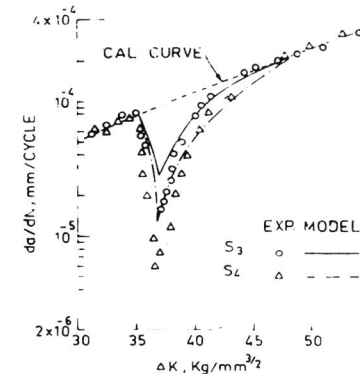Fig. 2   showing the variation of U Schematically
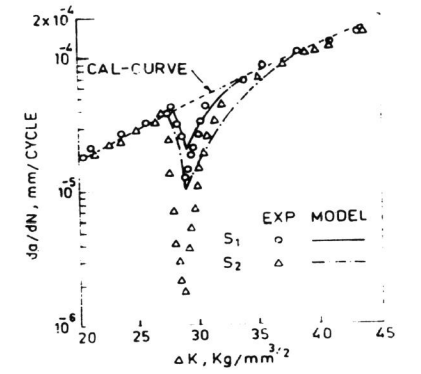
Fig. 3   comparision of model and experimental results of U

(a)   (b)

Fig. 4   Variation of da/dN w.r.t., ΔK for single PHLC in CAL test, S_1 to S_4

increases, the model results are found to be higher than the experimental results, showing the maximum difference at minimum crack growth rate values. On further increase in ΔK, the difference starts to decrease and disappears at ΔK = 29.75, 30.5, 38.0 and 40.25 kg/mm$^{3/2}$ for S_1 to S_4 tests or when the crack traverses 35-45% of a^*_{02}. For S_5 test, the model results agree closely with the experimental data (Fig.5).

The a/N curves (Figs. 6 and 7) show that the ratios of number of cycles found from CGR model (N_M) to those found experimentally (N_E) for S_1(PHLR = 1.5) and S_2 (= 2.0) tests (CAL = 5.40 kg/mm^2, R = 0.10) within the affecting zone are 74.10% and 38.0%, while upto failure same are 87.8% and 49.6 % respectively. These ratios for S_3(=1.50) and S_4(=1.75) tests (CAL = 6.75 kg/mm^2,
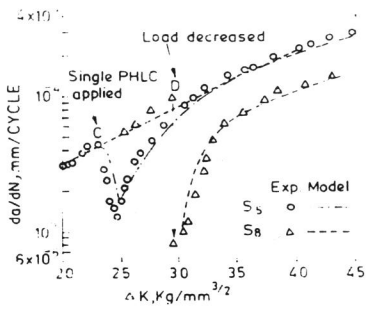
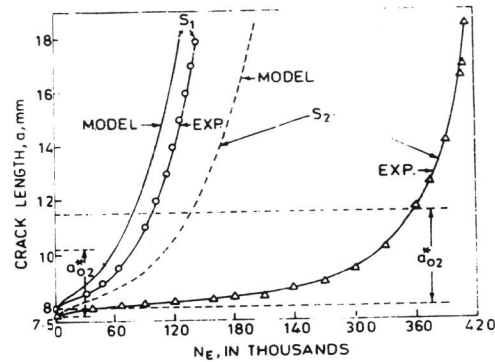Fig. 5 Variation of da/dN Vs ΔK for S_5 and S_8 tests

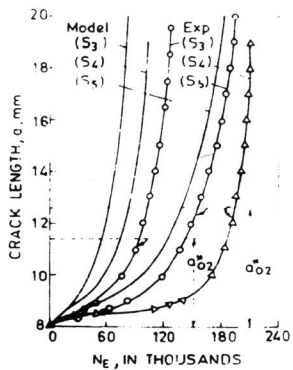Fig. 6 Crack length Vs number of cycles curves for S_1 and S_2 tests

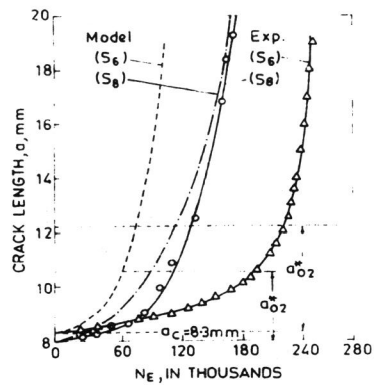Fig. 7 Crack length Vs number of cycles curves for S_3 to S_5 tests

Fig. 8 Crack length Vs number of cycles curves for S_6 and S_8 tests

Fig. 9

Fig. 10

Fig. 9 Variation of da/dN w.r.t. ΔK for Hi-Lo and Lo-Hi load sequence tests

Fig. 10 Crack length Vs number of cycles for multi PHLC in CAL tests

Intermediate multi PHLC tests. For this case, the model results are compared with literature data (Bell and Creager, 1974). The a/N curves (Fig.10) are developed using U-models (eqns.7) and CGR eqn.(1) for 2219-T 851 Al-alloy for N_{PH} = 2,5,10 (a_C = 23.10), 10 (= 27.60) and 20. The value of N_S for this alloy is 13 (Bell and Creager, 1974), so for N_{PH} = 20, the U-model of Hi-Lo load sequence (eqn.6) is used. It is evident from Fig. 10, that for N_{PH} = 2, 5,10 and 20, the model gives the percentage of N_M to N_E within the affecting zone as 62.0%, 52.3%, 50%, 50% and 45.3% respectively.

Lo-Hi load sequence test (S_7). As shown in fig. 9 the experimental CGRS show an acceleration after load change. On further crack extension, the same starts to decrease and merge with CAL-CGR of lower load level. The model results agree closely (within 12.0%) with those found experimentally.

Decrease in mean load test (S_8). The CGRS immediately after load change (Fig.5) abruptly decreases to a lowest value and thereafter starts to increase and merges in CAL- CGR curve of low load level, when crack traverses a_{02}^*. As shown in Fig. 8 the percentages of N_M compared to N_E within the affecting zone and upto failure are 93% respectively.

DISCUSSION

It is observed that total tests can be put in two categories as given below :

Tests S_1, S_2, S_3, S_4 and S_5. In these tests after load change from high to low, the residual deformations of fracture faces created by high loads seem to come in contact with each other and do not allow the newly created fracture faces to meet. Since this aspect is not considered, a shorter life is estimated by the model. With increase in PHLR and number of multi PHLC, the model results become more and more conservative, as crack tip blunting progressively increases.

Tests S_5, S_7 and S_8. In tests S_5 and S_8, the crack closure loads lie below

R = 0.10) within affecting zone are 62.1% and 43.6%, while upto failure 63.6% and 49.5% respectively. For S_5 (= 1.75) test (CAL = 4.5 kg/mm², R = 0.40), the ratios of N_M to N_E within the affecting zone and upto failure are 90.1% and 89.4% respectively.

Hi-Lo load sequence test (S_6). The value of PHLR for this test 1.75. Just after load change, the CGR-model results (Fig.9) are 1.8 - 2.0 times higher than the experimental data upto ΔK = 35.6 kg/mm$^{3/2}$ or till the crack traverses 40% of a_{02}^*. Thereafter, the difference between the two CGRS decreases and disappears at ΔK = 42.8 kg/mm$^{3/2}$ or when the crack traverses 1.10 times of a_{02}^*. From a/N plot (Fig.8), it is observed that percentages of N_M compared to N_E within the a_{02}^* and upto failure are 35.5% and 45.0% respectively.
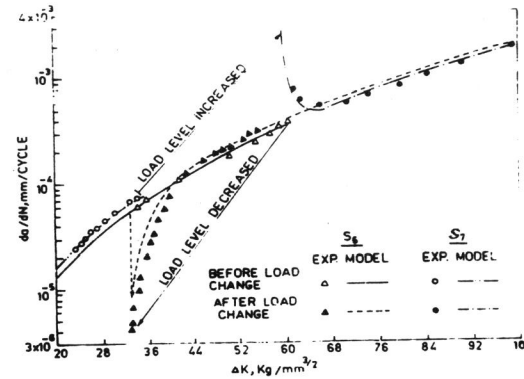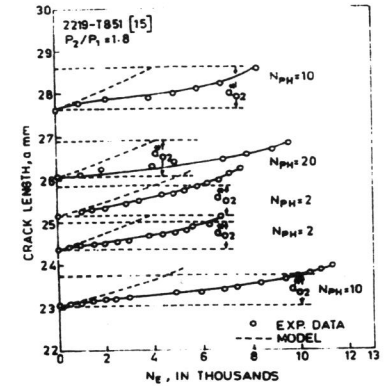
the level of minimum load. The crack therefore converts in the form of slit and old fracture faces do not meet during further cycling. A new crack starts from the end of the slit. Since, the new crack is sharp, there is no crack tip blunting. Because of evaluation of slit, no interference at the crack faces (crack tip slit) is encountered in further cycling and model results become applicable as the new crack is sharp. In S_7 test, there is no interaction effect of crack tip blunting, as after load change, the test is run at high load sequence.

The models of U developed for different load patterns given by eqn. (5), (6), (7) and (8) involve a power constant q. Since q is an exponent, its variation has appreciable effect on U. More work is required for relating q and U for different cases of variable amplitude loading. Particularly, the effect of crack tip conditions should be considered in the model.

CONCLUSIONS

1. The trend of variation of U and CGRS obtained from the present models in all the tests is observed to be similar to the variation of experimental CGRS.
2. The a/N results of present models lie within 35.5-97.0% of experimental results.
3. The model results for CAL- tests (R = 0.1) with single PHLC for a given load level, become more conservative as PHLR increases.
4. The model results, for CAL tests (R = 0.10) with multi PHLC and Hi-Lo load sequence tests, are on conservative side. The conservative trend exists upto a certain distance within plastic zone after load change.
5. For decrease in mean load test, Lo-Hi load sequence test and CAL test (R = .4) with single PHLC agree closely with those found experimentally.

ACKNOWLEDGEMENT

REFERENCES

Bell, P.D., and M. Creager (1974). AFFDL-TR-74-129.
Buck, O., J.D. Frandsen, and H.L. Marcus (1976). ASTM STP 595, 101-112.
Chand, S., and S.B.L. Garg (1983a). EFM8, 333-347.
Chand, S., and S.B.L. Garg (1983b). EFM, Accepted for publication.
Chand, S., and S.B.L. Garg (1983c). J. of Engng. Mat. and Tech.Trans. of ASME, (Communicated).
Elber, W. (1971). ASTM STP 486, 230-242.
Jones, R.E. (1973). EFM5, 585-604.
Mills, W.J., and R.W. Hertzberg (1976). EFM8, 657-667.
VonEuw, E.F.J., and R.W. Hertzberg (1972). ASTM STP513, 230-259.